



Single-sweep voltage-sensitive dye imaging of interacting identified neurons

Wolfgang Stein^a, Carola Städele^a, Peter Andras^{b,c,*}

^a Institute of Neurobiology, Ulm University, D-89069 Ulm, Germany

^b School of Computing Science, Newcastle University, Claremont Tower, Claremont Road, Newcastle upon Tyne NE1 7RU, UK

^c Institute of Neuroscience, Newcastle University, Henry Wellcome Building, Newcastle upon Tyne NE2 2HH, UK

ARTICLE INFO

Article history:

Received 2 September 2010
Received in revised form 8 October 2010
Accepted 8 October 2010

Keywords:

Voltage-sensitive dye
Stomatogastric ganglion
Neuron resolution imaging
Neuron interaction imaging

ABSTRACT

The simultaneous recording of many individual neurons is fundamental to understanding the integral functionality of neural systems. Imaging with voltage-sensitive dyes (VSDs) is a key approach to achieve this goal and a promising technique to supplement electrophysiological recordings. However, the lack of connectivity maps between imaged neurons and the requirement of averaging over repeated trials impede functional interpretations. Here we demonstrate fast, high resolution and single-sweep VSD imaging of identified and synaptically interacting neurons. We show for the first time the optical recording of individual action potentials and mutual inhibitory synaptic input of two key players in the well-characterized pyloric central pattern generator in the crab stomatogastric ganglion (STG). We also demonstrate the presence of individual synaptic potentials from other identified circuit neurons. We argue that imaging of neural networks with identifiable neurons with well-known connectivity, like in the STG, is crucial for the understanding of emergence of network functionality.

© 2010 Elsevier B.V. Open access under [CC BY-NC-ND license](https://creativecommons.org/licenses/by-nc-nd/4.0/).

1. Introduction

Simultaneous imaging of several or many neurons is a key approach to uncover how neural circuits and networks deliver their integral functionality as an emergent result of the interactions and activities of participating neurons (Grinvald et al., 1977; Zecevic et al., 1989; Wu et al., 1994; O'Malley et al., 1996; Obaid et al., 1999; Stosiek et al., 2003; Briggman et al., 2005; Dombeck et al., 2007; Frost et al., 2007; Orger et al., 2008; Yaksi et al., 2008; Mukamel et al., 2009; Rotschild et al., 2010; Briggman et al., 2010). Yet, at the same time knowledge of the underlying network connectivity and intrinsic properties of the network neurons is indispensable for determining the mechanisms that generate the network activity. One of the major endeavours in current neuroscience is thus to combine network connectivity and physiology with that of individual neurons. The connectivity within large networks is often unknown and single cell electrophysiology is insufficient to identify it due to the sheer number of neurons involved. On the other hand, many classical model systems have been studied on the single neuron level and connectivities in these networks are often well-described. However, the combined network activity, the network

level integral functionalities, and the control by higher centers are much more difficult to study with traditional recording techniques such as simultaneous intra- and extracellular recording of several neurons (e.g. Miller, 1987). The significant limitations here are due to physical limits on the spatial positioning of the electrodes. One of the biggest challenges today is to combine analysis at network and single cell level. This can be done in the most meaningful way in systems with identified neurons and well-established connectivity.

Here, we demonstrate the use of voltage-sensitive dyes to measure neural activity and neuronal interactions in a model system for motor pattern generation that has been thoroughly characterized on the single cell level, namely the crab stomatogastric ganglion (STG; Stein, 2009; Nusbaum and Beenhakker, 2002). The STG is a vital component of the crab nervous system and drives the rhythmic movement of muscles in the foregut (three internal teeth in the gastric mill of the stomach and the movements of the pyloric filter apparatus; Harris-Warrick et al., 1992; Nusbaum and Beenhakker, 2002; Marder and Bucher, 2007). All neurons in the STG are identified, as is their connectivity. STG neurons receive their input from higher ganglia through a single nerve (*stn*; Fig. 1A; Coleman et al., 1992) and deliver their function quasi-autonomously, i.e. they form central pattern generators (CPGs) which are located in the STG itself (Marder and Weimann, 1992; Nusbaum and Beenhakker, 2002). The activity of many, but not all, STG neurons can be recorded and identified extracellularly from motor nerves that originate from the STG to determine the mode of function (or system functionality or behaviour) of the STG (Harris-Warrick et al., 1992). Synaptic

* Corresponding author at: School of Computing Science, Newcastle University, Claremont Tower, Claremont Road, Newcastle upon Tyne NE1 7RU, UK. Tel.: +44 191 2227946; fax: +44 191 2228232.

E-mail address: peter.andras@ncl.ac.uk (P. Andras).

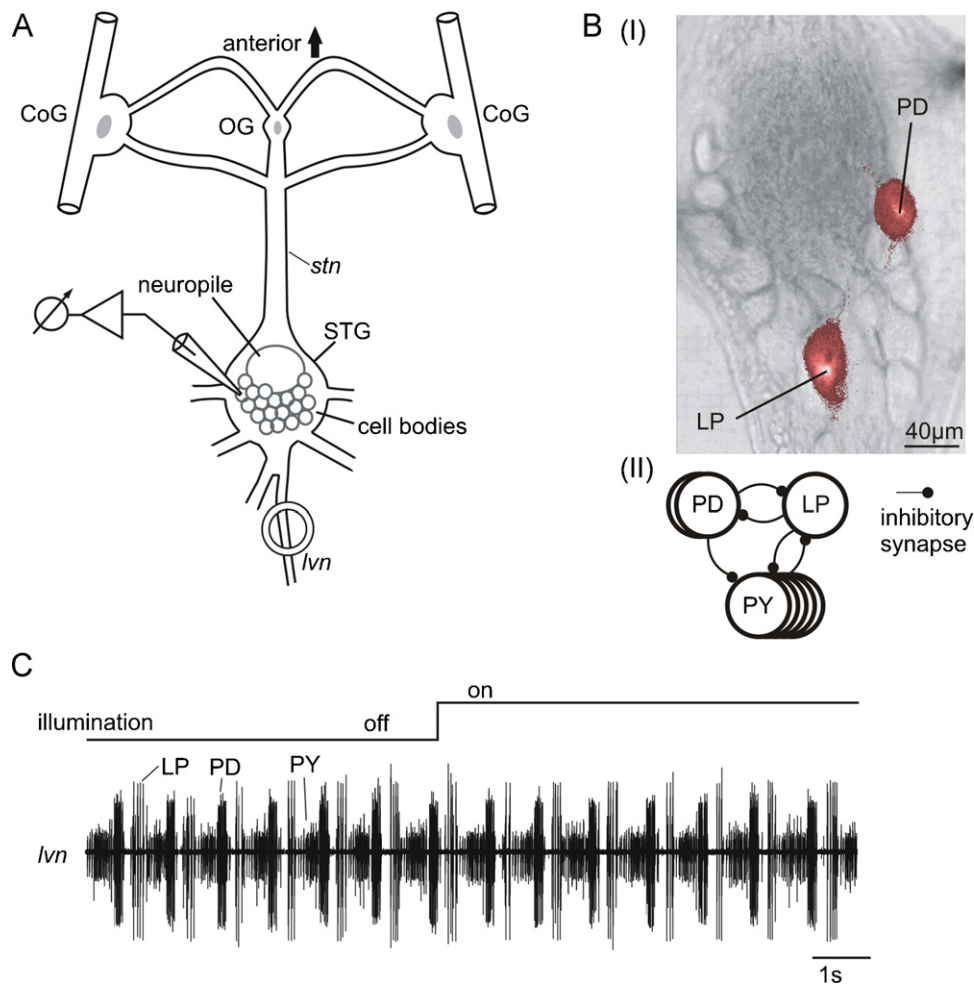


Fig. 1. (A) Schematic drawing of the STNS showing the location of the STG neuron cell bodies and the experimental approach. Neurons were impaled and recorded with sharp microelectrodes and filled with di-8-ANEPPQ. CoG: commissural ganglion; OG: esophageal ganglion; STG: stomatogastric ganglion; stn: stomatogastric nerve; lvn: lateral ventricular nerve. (B) (I) Photo of the STG in bright field and overlay of two neurons (LP and PD) stained with di-8-ANEPPQ and visualized in fluorescent light. PD: pyloric dilator neuron; LP: lateral pyloric neuron. (II) Simplified representation of the connectivity between PD, LP and PY neurons. PD and LP as well as LP and PY are connected via reciprocal inhibition. PY: pyloric constrictor neuron. (C) Excitation with fluorescent light did neither affect network nor single cell spike activity after filling PD and LP neurons. Extracellular recording of the *lvn*, showing the rhythmic activity of LP, PY and PD during the pyloric rhythm. Average (12 cycles) period of the pyloric rhythm before illumination: 1.85 ± 0.1 s, during illumination: 1.81 ± 0.2 s. Mean number of LP spikes before illumination: 3.75 ± 0.6 , during illumination: 3.58 ± 0.8 . LP duty cycle before illumination: 0.14 ± 0.04 , during illumination: 0.13 ± 0.04 . LP spike frequency before illumination: 10.62 ± 1.2 Hz, during illumination: 10.93 ± 2.9 Hz. PD duty cycle before illumination: 0.15 ± 0.01 , during illumination: 0.15 ± 0.03 . Other parameters for PD and PY could not be determined from the extracellular recording since it contains the action potentials of several PD and PY neurons.

interactions and ion channel activities are typically studied using intracellular recording techniques (Harris-Warrick et al., 1992; Marder and Bucher, 2007). There are two principle restrictions to these approaches: (1) the number of such recordings is limited by the space needed to place micromanipulators and electrodes (e.g. Miller (1987) reports the use of four intracellular electrodes simultaneously); (2) synaptic and ionic currents are recorded with sharp microelectrodes in the soma and thus electrotonically relatively far from the neuropile, in which most of the processing in these neurons is accomplished, thus leading to attenuation of the recorded signals. Optical imaging may offer a solution to both problems: for example, calcium imaging has been applied successfully to analyse the processing within individual STG neurons following loading of the selected neuron with calcium dye (Graubard and Ross, 1985; Ross and Graubard, 1989). Yet, calcium dyes lack the appropriate time resolution to observe quick neural events and only act as indirect reporters for changes in membrane potential. In principle, the STG is an ideal system for simultaneous optical imaging of many neurons, because its 26 neurons are arranged in a flat crescent or semi-circle shape in the posterior part of the ganglion.

Here we report for the first time the simultaneous recording of STG neuron activity with traditional intra- and extracellular recordings and optical imaging of membrane potential changes using voltage-sensitive dyes (VSDs). This technique opens the avenue for the systematic analysis of processing within individual neurons and of the multi-neuron activity of a pattern generating circuit whose connectivity and intrinsic properties have been well characterized. Pioneering the analysis of neuronal activities on both single cell and network levels will have major impact on STG research, but also on a wide range of areas of neuroscience research: the STG is a prototype system of CPG networks (containing two separate, but interacting CPGs – the pyloric and gastric mill circuits) and as such the understanding of its emergent system level properties will improve the understanding of CPG networks in general. Such CPG networks being at the heart of vital systems such as movement generation, coordination (Grillner, 2006; Goulding, 2009) and respiration (Ramirez and Richter, 1996), better understanding of how they are organized and deliver their system level functionality may have a major impact on a wide range of neuroscience research related to motor control, but also to that concerned with cognitive functions (Yuste et al., 2005).

2. Materials and methods

2.1. Dissection

Adult *Cancer pagurus* L. were obtained from local sources (Newcastle University, Dove Marine Laboratories) and kept in filtered, aerated seawater (10–12 °C). Altogether, more than 20 preparations were used. Animals were anesthetized by packing them in ice for 20–40 min before dissection. We used isolated nervous systems to perform our experiments (Gutierrez and Grashow, 2009). The STNS was pinned down in a silicone elastomer-lined (ELASTOSIL RT-601, Wacker, Munich, Germany) Petri dish and continuously superfused (7–12 ml/min) with chilled saline (10–13 °C; Fig. 1A). Physiological saline consisted of (mMol l⁻¹): NaCl, 440; MgCl₂, 26; CaCl₂, 13; KCl, 11; trisma base, 10; maleic acid, 5. Saline was kept at a constant temperature of 11–13 °C and at pH 7.4–7.6. All experiments were carried out in accordance with the European Communities Council Directive of 24th November 1986 (86/609/EEC).

2.2. Intracellular and extracellular recording

We used standard methods to perform electrophysiology (Bartos and Nusbaum, 1997; Blitz and Nusbaum, 1997; Stein et al., 2006). We desheathed the STG to facilitate intracellular recordings. Glass electrodes (GB 100TF-8P, Science Products, Hofheim, Germany; 25–40 MΩ) filled with 3 M KCl solution were used. Signals were amplified using a BA 01X Amplifier (NPI, Tamm, Germany) (in bridge mode and digitized using an NI PIC 6220 (National Instruments, Austin, TX, USA). Files were recorded and saved using WinEDR v2.9 (Strathclyde Electrophysiology Software; University of Strathclyde, Glasgow, UK). Files were then converted and analysed using Spike 2 v6.10 (Cambridge Electronic Design, Cambridge, UK). The signal was also recorded with the MiCAM02 imaging system (SciMedia Ltd., Tokyo, Japan; using the analogue input; see below). For extracellular recordings, a petroleum jelly-based cylindrical compartment was built around a section of the nerve to electrically isolate STNS nerves from the bath. One of two stainless steel electrode wires was placed in this compartment, the other one in the bath as a reference electrode. The differential signal was recorded, filtered and amplified with an AC differential amplifier (Univ. Kaiserslautern, Germany). Activity patterns and axonal projection pathways were used to identify STG neurons, as described previously (Heinzel et al., 1993; Bartos and Nusbaum, 1997; Blitz and Nusbaum, 1997).

2.3. Preparation of the dye and electrode loading

VSDs are lipophilic molecules that are anchored inside the neuronal membrane. Several different types exist (Loew, 1996) and, depending on the type, they report the changes in membrane potential using different mechanisms. We used fluorescent dyes and epifluorescence imaging, which have some advantages compared to other kinds of dyes (e.g. the signal is larger than in the case of absorption dyes (e.g. Zecevic et al., 1989), and only a single kind of dye molecule is required and not two as in the case of FRET dyes (e.g. Briggman and Kristan, 2006)). The toxicity (especially phototoxicity) of the dyes may be an issue in optical imaging. We tested earlier the sensitivity of the crab STG in the context of epifluorescent optical imaging with ANEP dyes (Stein and Andras, 2010) and we found that they had no sustained toxic effect on STG neurons.

We used di-8-ANEPPQ (Cambridge Bioscience, Cambridge, UK) and applied it using intracellular iontophoretic injection with sharp microelectrodes. For this, the tips of standard glass microelectrodes with filament were filled with the dye: the stock solution of di-8-ANEPPQ was made by mixing 5 mg dye with 1 ml 20% F-127

pluronic acid DMSO solution (Invitrogen, Paisley, UK) (resulting dye concentration: 6.97×10^{-3} M) and then centrifuged for 20 min at 12,000 rpm with an Eppendorf Centrifuge 8504 (Eppendorf, Hamburg, Germany) to separate larger particles in the dye stock solution that may cause clogging of the microelectrode. The supernatant was used for filling the electrodes: a droplet was injected into the electrode and placed close to the tip using a MicroFil (34 gauge; WPI, Berlin, Germany) needle. Following this the glass electrode was backfilled with 3 M KCl solution and placed in a dust-protected chamber for at least 1 h to allow diffusion of the dye into the tip. Electrodes resistances were typically between 30 and 50 MΩ. Electrodes above 50 MΩ and below 20 MΩ were discarded. After successful impalement and identification of the neuron, the neuron was filled with the dye. Pulses of 10 nA positive current with a duration of 1.5 s and 1.5 s interpulse duration were used to drive the dye molecules into the cell. We used positive current because the di-8-ANEPPQ dye molecules have a double positive charge (in solution, the di-8-ANEPPS molecule forms an ionic mix with two Br⁻ ions per dye molecule). The loading procedure lasted 20–30 min per neuron and resulted in a bright staining of the soma and the primary neurite (Fig. 1B).

2.4. Imaging of fluorescence

For the fluorescence imaging we used a MiCAM 02 imaging system (SciMedia Ltd., Tokyo, Japan) using the HR (high resolution) camera (6.4 mm × 4.8 mm actual sensor size) set at 96 × 64 pixel spatial resolution, 2.2 ms temporal resolution and a 20× objective (XLUMPLFL20XW/0.95, NA 0.95, WD 2.0 mm; Olympus Corporation, Tokyo, Japan) mounted on a standard upright fluorescence microscope (BX51 WI, Olympus Corporation, Tokyo, Japan) or the same camera and objective but having the camera settings at 48 × 32 pixel spatial, resolution and 1.5 ms temporal resolution. The illumination was provided by a 150 W ultra-low ripple halogen light source (HL-151, Moritex Corporation, Tokyo, Japan) with computer controlled shutter. To get the exciting green light we used a wide green filter cube (480–550 nm excitation filter, MSWG2, Olympus Corporation, Tokyo, Japan).

2.5. Data analysis and visualization

For data analysis and visualization we used the BrainVision software (SciMedia Ltd., Tokyo, Japan) associated with the MiCAM02 imaging system. Final figures were prepared with CorelDraw (version 12 for Windows, Corel Corporation, Ottawa, ON, Canada). Graphics and statistics were generated using Excel (Microsoft). The cycle period of the pyloric rhythm was defined as the duration between the onset of a PD neuron burst and the onset of the subsequent PD burst. Burst durations were defined as the time between the first and last action potential (spike) within a burst.

3. Results

3.1. Simultaneous intracellular and optical recording of neural activity as a proof of concept

Imaging analysis of STG neurons so far was limited to the use of calcium dyes (Graubard and Ross, 1985; Ross and Graubard, 1989) that allow only indirect tracking of membrane potential variations. In contrast, fluorescent VSDs allow a much quicker (in the millisecond range) and more direct detection of membrane potential changes, since they reside within the cell membrane and their fluorescence depends on the voltage difference across the membrane. Yet, imaging of STG neurons remained elusive due to various problems with dyes that were tried (e.g. toxicity, lack of effective loading).

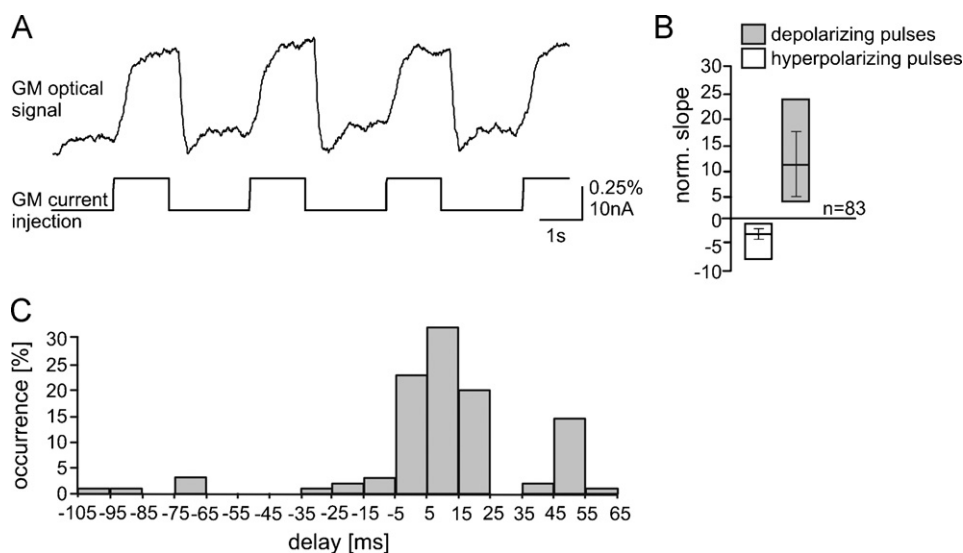


Fig. 2. (A) Optical recording of a gastric mill (GM) neuron during current injection with the microelectrode. (B) The slope of the optical signal corresponding to the direction of the current injection in all instances. Slope was normalized by first eliminating the trend from the data series (the trend is occasionally present in the data series, showing a gradual increase or decrease of all data values), and then scaling the data to be in the same value range for all data series, and also considering the different temporal resolutions that we used for data acquisition. The box plot gives minimum and maximum values, as well as mean and standard deviation. (C) Time delays (in ms) between the start times of the current pulses and the corresponding changes in the optical recording. Extreme outliers (>65 ms) were ignored.

Here, to perform VSD imaging, we loaded individual STG neurons intracellularly with di-8-ANEPPQ VSD (see Section 2 and Fig. 1B). We did not see any obvious toxic effects following the loading procedure and during the experiments ($n > 10$ imaging sessions, each over a few hours period): the neurons kept their regular activity, i.e. their duty cycle and phase relationship within the pyloric rhythm remained constant, as was action potential firing (Fig. 1C).

To test whether di-8-ANEPPQ fluorescence changed with the membrane potential of the recorded cell, we first drove the membrane potential of the neuron with pulsed current injections of several nA (de- and hyperpolarizing pulses). The variation of the optical signal recorded from the dye-filled neurons followed closely the current injection. Fig. 2A shows an example of a GM (gastric mill) neuron recording. The GM neurons are particularly well suited for these tests since they participate in the gastric mill rhythm, which is episodic and often absent in isolated preparations (in contrast to the pyloric rhythm; Stein, 2009). The GM neurons thus typically show tonic activity and their membrane potential can easily be changed with current injections. We quantified the response on the optical signal in two ways: (1) in each trial we measured the slope of the optical signal when the membrane voltage was at the mid-point between the corresponding maximum and minimum values. We found that in all instances ($n = 83$) the slope in the change of the optical signal corresponded to that of the current pulse (Fig. 2B); (2) we measured the difference between the time of switching the polarity of the driving current and the time when this switch was indicated by the change in the optical recordings (Fig. 2C). To measure this latency, we considered the times of the midpoint of the transition between the high and low value recordings of the current and of the optical signal recorded from the neuron (Fig. 2A) and binned the values in 10 ms bins. 75.9% of all switches in the optical signal occurred within 25 ms after the current stimulus changed polarity. On average the time delay was 15.17 ± 19 ms ($n = 83$). This confirmed that the di-8-ANEPPQ responded reliably and with detectable changes in fluorescence to membrane potential changes in STG neurons.

After this first step, we applied hyperpolarizing current pulses, which in most neurons induced rebound spikes after release from inhibition. The simultaneous optical and intracellular recordings show that even single action potentials could be detected with

very good match by the optical recording. Fig. 3A shows an example of the simultaneous optical and intracellular recordings of a GM neuron. Note that we did not apply any averaging over multiple spike recordings or rebound trials, but rather single-sweep imaging of neural activity. We calculated the start, end and peak times for recorded spikes both from the optical and the electrical signal, and the duration of the spikes as well in both cases. The distributions of the difference between corresponding time values (e.g. the difference between voltage recording start time of a given spike and optical recording start time of the same spike) are shown in Fig. 3B–E. These show that indeed, the difference value distributions are centred around or below 1 ms with a narrow variance, i.e. on average the difference of spike peak times was 0.91 ± 1.37 ms ($n = 18$), the difference of spike start times was 0.58 ± 3.49 ms ($n = 18$), the difference of spike end times was 1.08 ± 4.45 ms ($n = 18$), and the average difference of durations was 0.5 ± 5.37 ms ($n = 18$). This confirmed that optical and electrical recording of spikes were well matched and that di-8-ANEPPQ reported changes in the membrane voltage with only a very short delay. We also calculated the correlation between voltage recordings of induced spikes and the corresponding optical recordings of the neural activity (Fig. 3F). This analysis shows that the two readings are well correlated with a correlation coefficient $r = 0.6893$ ($p < 0.001$, $n = 351$ data points).

An important application of VSD imaging is to investigate signal processing within a given neuron. As a first step, we thus compared the optical signals obtained from the neuron's soma with those from the neuron's primary neurite. Fig. 4 shows the results for an LP neuron. Both, the single-sweep recordings and the average show the correlated activity in the soma and the neurite (Fig. 4A and B). In the STG, action potentials are generated in the axon and passively invade the soma (the spike initiation zone is outside of the soma in the part of the axon that is within the ganglion; the action potentials have to pass through the primary neurite in order to reach the soma). Correspondingly, we found a clear delay between the peaks of the action potentials in soma and neurite. On average, action potentials occurred 3.52 ms ($n = 48$) earlier in the neurite than in the soma (Fig. 4C).

Our data thus demonstrates that high temporal and spatial resolution VSD imaging of STG neurons is possible and that the

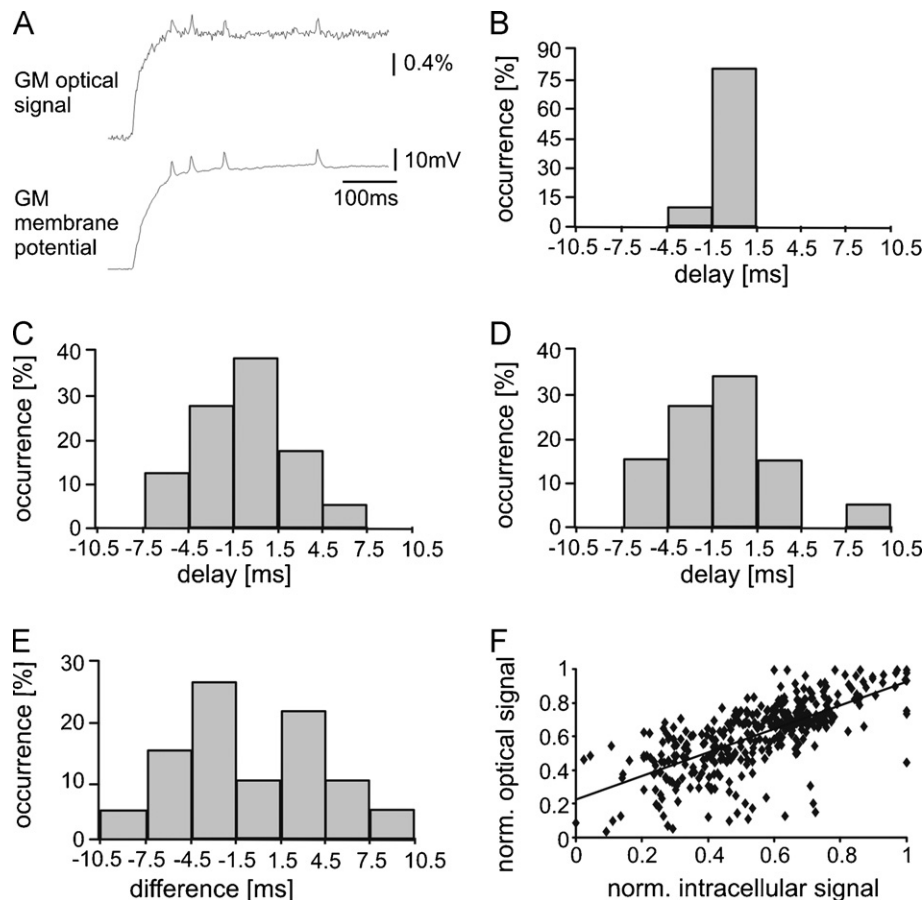


Fig. 3. (A) Simultaneous intracellular and optical recordings of a rebound from inhibition in a GM neuron. GM fires 4 action potentials during the rebound which are all clearly visible in the optical signal. Distributions of the delays between voltage recording of a given action potential and optical recording. (B) Action potential peak, (C) start times, (D) end times, (E) difference of duration. (F) Correlation between membrane potential changes during action potentials and the corresponding optical recordings ($n = 351$, slope: 0.70, $r = 0.6893$; significantly different from zero with $P < 0.05$; Pearson product-moment correlation and subsequent t -test).

recorded fluorescence signals follow very closely the membrane potential variation of the neurons, both in the soma and the neurite. More importantly we demonstrate that it is possible to do single-sweep recording of spiking activity of neurons, without the need for averaging over many spiking events or trials. This means that this method allows following of the activity of individual neurons in instant detail, without requiring repetition of the experimental conditions (such as neuronal or sensory stimulation, for example).

3.2. Single-sweep optical recordings of synaptically interacting identified neurons

The activity produced by a network is generated by both intrinsic neuron properties and synaptic connections. Recent studies have shown that both are under neuromodulatory control and that neuromodulator actions are essential to determine the network activity (Marder and Thirumalai, 2002), even in the long term (Khorkova and Golowasch, 2007; Zhao et al., 2010). For example, the strength of the sole feedback synapse from the pyloric network to the pacemaker kernel, namely that between the lateral pyloric neuron (LP) and the pyloric dilator (PD) neurons, is altered by a peptide modulator (RPCH; Thirumalai et al., 2006). While simultaneous intracellular recordings of several STG neurons are possible, there are space limitations that impose a limit on how many neurons can be recorded and time limitation that restrict the maximum time of a recording (for example due to manipulator drift or leakage of electrode electrolyte into the cell). For proper understanding of how a network of neurons delivers its system level functionality

many (ideally all) neurons and their synaptic interactions should be recorded individually and simultaneously, over an extended period of time.

Here, we demonstrate a one-by-one filling of an LP and a PD neuron with di-8-ANEPPQ and a subsequent optical recording of their interacting activity. LP and PD neurons are essential for generating the pyloric rhythm and are connected with a reciprocal synaptic inhibition. Here, we identified them on the basis of their intracellularly recorded individual activity pattern and the relationship of their intracellular activity to the extracellular recordings of the lateral ventricular nerve (*lvn*) (Heinzel et al., 1993; Bartos and Nusbaum, 1997; Blitz and Nusbaum, 1997). Using these neurons will allow us to determine both the feasibility of optical recordings to measure the activity of several neurons simultaneously and to determine synaptic interactions between them.

After successive filling of both neurons (Fig. 1B), we removed the intracellular electrodes and started the simultaneous optical recording of both neurons. We compared the optical signal to their spike activity recorded extracellularly on the *lvn*, on which LP and PD spikes can easily be separated. They occur in bursts at identifiable phases during the pyloric rhythm (Fig. 1C; Stein, 2009). Examples of the optical recordings are shown in Fig. 5A.

Our recordings show that in regularly bursting neurons we could clearly identify spikes and membrane potential oscillations. In fact, the phase relationship between PD and LP could easily be detected (Fig. 5A and E; see also supplementary Movie S1): LP and PD showed alternating peaks of activity in the optical recording, as expected from the spike activity on the *lvn*. When we compared the period of

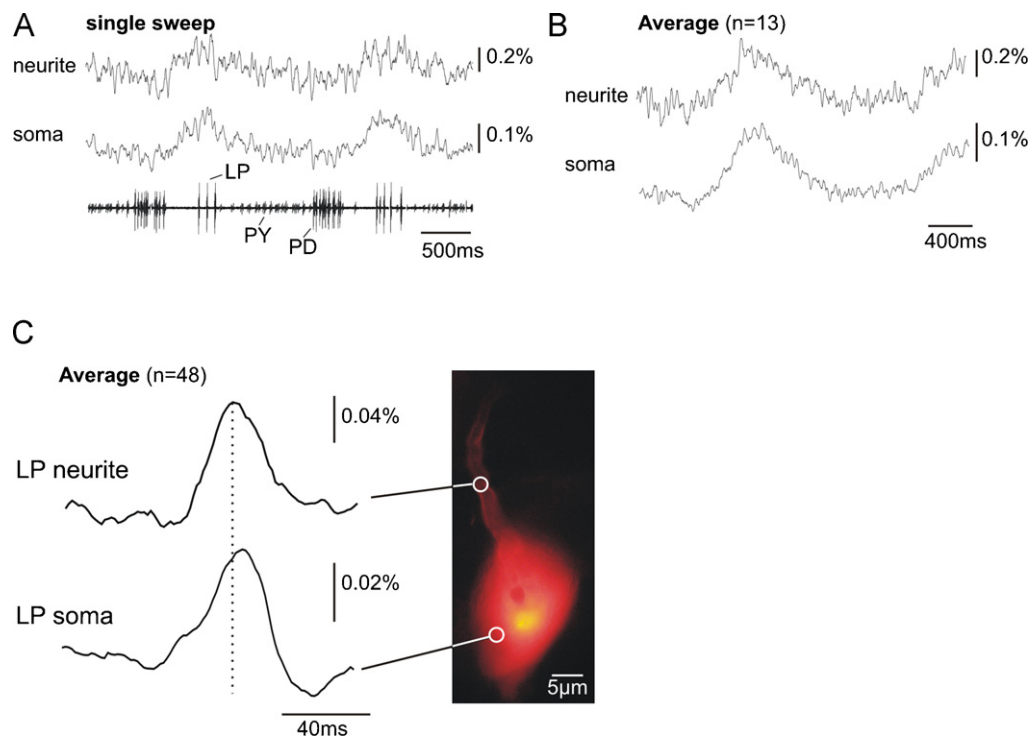


Fig. 4. (A) Simultaneous single-sweep optical recordings from LP soma and primary neurite (for location see (C)) along with extracellular recording of the *lvn* showing the spike activity of PD, LP and PY neurons. (B) Average of optical signals from soma and neurite. The duration of one pyloric cycle is shown. (C) Left: average of action potentials measured in soma and neurite (note the difference in the time scale in comparison to (B)). Action potentials detected on the extracellular recording were used to trigger the average (not shown). The peak of the action potentials occurred earlier in the neurite, indicating that action potentials were generated in the axon or neuropile and subsequently invaded the soma via the primary neurite. Right: photo of LP. The circles indicate the locations where the optical signals were recorded from.

the pyloric rhythm measured from the optical signal with that measured from the spike activity on the *lvn*, we found that they were virtually identical (*lvn*: 1.51 ± 0.09 s ($n = 16$); optical: 1.50 ± 0.09 s ($n = 15$)). The appropriately separated spiking activity of the two interconnected neurons was also clearly identifiable on the optical recordings from their soma and primary neurite and corresponds to that of the extracellular recording on the *lvn* (Figs. 4–6). To quantify the match between optically and electrically recorded spikes we calculated the differences between the times of the optically and extracellularly measured spike peaks. The distribution of the difference values is shown in Fig. 5B. The delay between optically and extracellularly measured spikes was centered around their average value 12.57 ± 3.96 ms ($n = 34$). The non-zero average value corresponds to the time delay between the arrival of the action potential in the soma and its arrival at the axon site in the *lvn* from where we recorded extracellularly. The delay corresponded well to that measured with intracellular electrodes (12 ms), before we removed the electrode from the soma. In Fig. 5C and D several sweeps of both, optical LP and PD spikes and those of the corresponding spikes on the *lvn* are shown, along with the average, demonstrating the small variation in the optical signal.

Besides spike activity, the recordings also show the mutually inhibitory effect of LP and PD on each other. While PD is part of the pacemaker kernel and its oscillations are generated by endogenous properties, LP oscillations depend on synaptic inhibition (and subsequent rebound) from PD (Nusbaum and Beenhakker, 2002; Stein, 2009). Yet, as most synaptic actions in the STG, the PD to LP synapse shows graded synaptic transmission, i.e. even subthreshold membrane potential of PD affect the postsynaptic LP cell (Hooper and DiCaprio, 2004). This was also clearly visible in the optical signal when we compared the average waveform of both LP and PD, in which LP started to hyperpolarize even before the PD reached its peak depolarization (Fig. 5E, arrow). This rather slow hyperpolar-

ization of LP due to the graded synaptic effect of PD was even visible in single-sweep recordings of LP (Fig. 6A). In addition to identifying these slow inhibitory postsynaptic potentials (IPSPs), we also monitored the occurrence of other synaptic inputs in LP, again without time averaging (Fig. 6A and C). These originated from the pyloric constrictor neurons (PY), which possess an inhibitory connection to LP (Fig. 1B, II). In fact, the optical signal closely mirrored the waveform of the LP membrane potential typically obtained during intracellular recordings (Fig. 6B) and individual PY–IPSPs could be seen in the optical recording. Fig. 6D shows an overlay of several single sweeps plus average of optically recorded PY–IPSPs and the closest PY spike recorded in the *lvn*. The PY induced IPSPs in the LP neuron are very clearly identifiable by averaging over several detected PY spikes (Fig. 6E). The averaging also shows the time delays of consecutive IPSPs caused by PY neuron activity – the multiple IPSP peaks represent the effect of the summing of temporally close PY spikes. These data thus demonstrate that even single synaptic events can reliably be detected with optical recordings.

4. Discussion

4.1. Optical recording of neurons in identified circuits

Optical recording of network activity with calcium- or voltage-sensitive dyes is one of the cutting-edge techniques used to measure the activity of large populations of neurons. Since the mid 1990s a growing number of papers have been published about the use of calcium imaging at neuron resolution that also allows the detection of simultaneous spiking activity of many neurons (up to around 100 neurons) (O'Malley et al., 1996; Stosiek et al., 2003; Dombeck et al., 2007; Greenberg et al., 2008; Holekamp et al., 2008; Kerr et al., 2007; Ohki et al., 2005; Yaksi et al., 2008; Mukamel et al., 2009; Rotschild et al., 2010). While calcium imaging allows

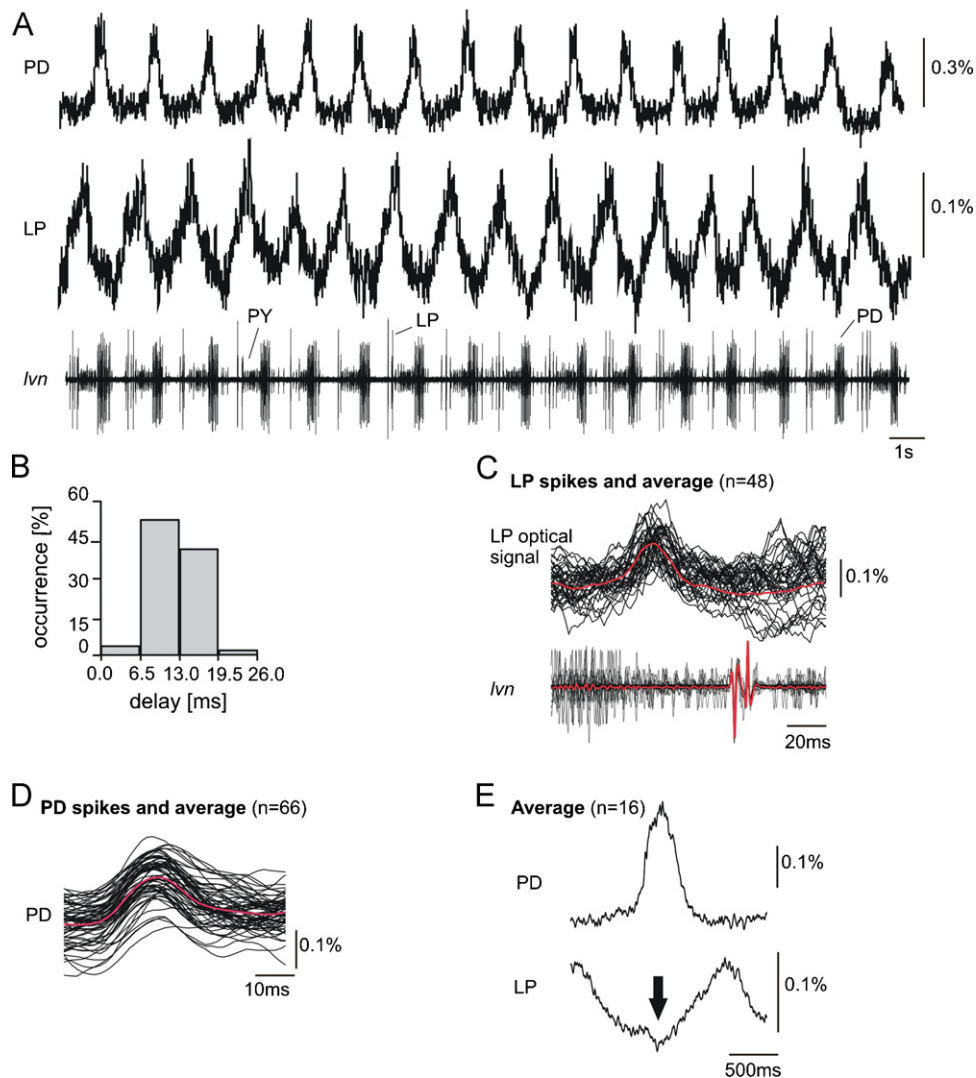


Fig. 5. (A) Simultaneous single-sweep optical recordings of LP and PD neurons, along with their extracellularly recorded spike activity on the *lvn*. (B) Distribution of delays between the peak of optically detected action potentials and extracellularly measured spike activity on the *lvn* – see also [supplementary Movie S1](#). (C) Single sweeps and average (red) of LP spikes on the *lvn* (bottom) and in the optical signal (top). The average was triggered on the LP spikes on the *lvn*. (D) Average of optically detected PD spikes. Since the spike activity of the two PD neurons is recorded on the *lvn*, i.e. there is an ambiguity in the identity of the PD spikes. Action potentials here were triggered using the clearly detectable peaks in the optical signal. (E) Average of the slow waveform of the PD and LP optical signals. The arrow indicates the slow inhibition received by LP, which is caused mostly by graded synaptic release from PD.

the inference of spiking activity, it is an indirect method that works best if the neurons fire single action potentials at low frequencies and the reliability of spike detection decreases as the number of spikes in a burst over short time period increases (Milojkovic et al., 2007). In contrast, VSDs are much faster and directly report changes in the membrane potential. VSDs have been promising to supplement or even replace electrophysiological recordings of membrane voltages for over two decades now. The first results about simultaneous imaging of neurons with VSDs were published in the late 1970s (Grinvald et al., 1977). Yet, most functional applications have targeted the measurement of population activities, i.e. the summed activity of whole brain areas rather than the membrane potential of single cells. In particular examples of imaging studies of individual neurons embedded in a functional neural circuit with known function and identifiable and synaptically interacting neurons are rare (Frost et al., 2007; Briggman et al., 2010). Even the detection of single action potentials in identified neurons has mostly been shown exemplary, for instance in the squid axon or the giant metacerebral neurons in snails (Baker et al., 2005).

An important problem of simultaneous optical imaging of neurons is the interpretation of the data, i.e. how can the recorded data be used to unveil the integration of individually recorded neural activities into the overall functionality of the network(s) to which these neurons belong. A principal underlying problem is often that the connectivity pattern of the imaged neurons is not known (i.e. it is known that the imaged neurons belong to a large network, but the topology of the network is not known), which is why in most experiments action potentials were elicited with current injections and thus showing little advantage over intracellular recordings with microelectrodes and revealing only limited functional conclusions. One approach to deal with the data interpretation problem is to induce functional behaviour in the network by stimulation and associate neural activities to induced function by analysing the correlation of recorded activities of neurons and the stimulus inducing the behaviour or hallmarks of the behaviour that can be recorded from the whole system (e.g. by extracellular recordings from nerves) (Cacciatore et al., 1999; Briggman et al., 2005; Wu et al., 1994; Orger et al., 2008; Rotschild et al., 2010; Ohki et al., 2005). Another approach is to infer the functional con-

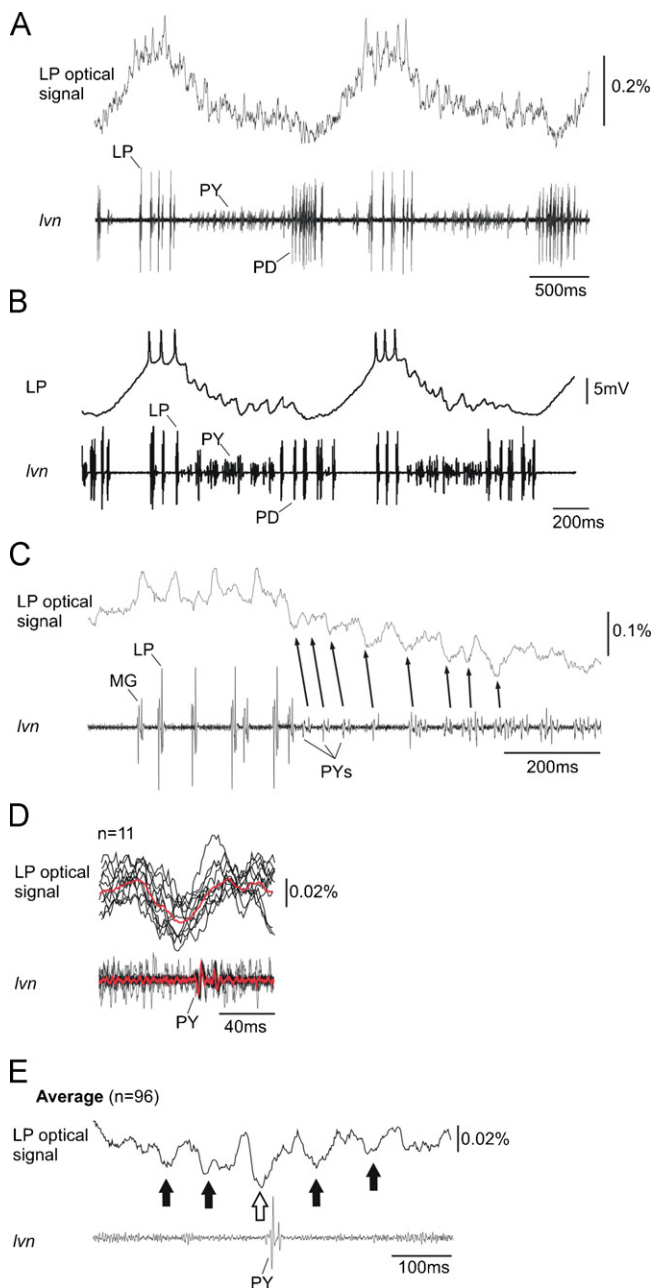


Fig. 6. (A) Single-sweep optical recording of LP during two pyloric cycles and corresponding extracellular recording of the *lvn*. LP spikes as well as synaptic inputs are clearly visible in the optical signal. (B) Intracellular recording of LP (different preparation) demonstrating the membrane potential changes in LP during two pyloric cycles. Note the similarity to the optical signal in (A). (C) Magnification (single sweep) of the LP optical signal. After the end of LP's spike activity, several IPSPs arrive that can be attributed to the PY spikes on the *lvn* (arrows). There are several PY neurons (Stein, 2009). Hence, since the conduction velocities between the different PY neurons vary to some extent, PY action potentials arrive with varying delays at the *lvn* recording site, which in turn results in arrows with different angles. (D) Single sweeps and average (red) of the optically recorded IPSP in LP and the corresponding PY spikes on the *lvn*. The *lvn* action potentials of a particular PY neuron were used for triggering. (E) Average triggered on all PY neuron spikes, demonstrating the timing of the corresponding IPSP in the optical signal (outlined arrow) and those of surrounding PY neurons (black arrows).

nectedness of imaged neurons (or groups of them) for example by analysing the correlations of firing patterns of the imaged neurons (e.g. Greenberg et al., 2008).

In principle, optical imaging with voltage-sensitive dyes faces the same problems that early electrophysiology had, namely that

a functional analysis of neural activities requires the knowledge of the connectivity in the underlying circuit (which is difficult to determine with optical recordings). Ideally, in order to determine and understand how individual neural activities organize into spatio-temporal patterns and through this deliver the functionality of the network(s) to which they belong, the activities of individual neurons should be recorded in neural systems where the functional connectivities and neuronal interactions are known and the system functionality is easy to identify through additional electrophysiological recordings of the system output. In principle, if these conditions are satisfied, it should be relatively straightforward to derive a valid interpretation of how individual neural activities lead to the emergence of system level behaviour and functionality.

Yet, in particular electrophysiologists face several problems which may contribute to the lack of functional approaches: (1) to put the optical signal in a functional context, control recordings with electrophysiological methods are required, but they are limited by the small distance between neurons and objective which makes difficult to place electrodes; (2) for the same reasons (electrode placement and control recordings) and also because of possible lack of tissue transparency, upright microscopes and illumination from the top (epifluorescence rather than absorption dye methods) are preferred; (3) a good match between the optical signal and the morphology of the recorded neurons is required. This is particularly important in circuits in which single cells are already identified and their morphological characteristics are used to determine their identity, such as in most classical model system preparations. Only recently the development of high-speed and low-noise cameras has allowed to replace low-resolution photodiode arrays (Baker et al., 2005); (4) in the light of current approaches to study functional aspects of neural activities that include variable and non-repetitive stimuli (for example in *in vivo* conditions) it is important to achieve a direct measurement of single action potentials or even synaptic inputs without the need for extensive averaging over many trials. Demonstrating the continuous measurement of current injections from -100 mV to $+150$ mV is thus not sufficient, but that of individual action potentials is. Thus, the optical signal and the recording device have to be fast and sensitive to small membrane potential changes; (5) in addition, the toxicity of the VSDs is often a problem, especially when high light levels are required. Also, since VSDs are often charged molecules they may change the electrical properties of the neurons (such as capacitance; Sjulson and Miesenbock, 2008), which is particularly unfortunate during long-term recordings; (6) only if simple ways to apply VSDs and to read the optical signal are available, researchers will be ready to pay the high prices for the microscope and camera equipment (about 10 times that of a good intracellular amplifier). It will also allow them to use these techniques themselves rather than having a separate expert in the lab. This is where our study comes into play. We are using simple dye injections that have been routinely used for other dyes in most physiology labs. Consecutive staining of several neurons is also a standard method. We demonstrate the optical recording of two synaptically interacting neurons – their firing activities and their synaptic potentials – in their functional context, i.e. without artificial stimulation (Fig. 5). No extensive averaging is necessary to detect synaptic input and action potentials. Since all neurons in the STG are identified (Nusbaum and Beenhakker, 2002; Marder and Bucher, 2007; Stein, 2009), the impalement with microelectrodes to inject the dye is sufficient to detect which neuron is filled with the dye and cells can easily be separated by the location of their somata (an advantage of the CCD camera system over photodiode arrays).

The advantage of recording neurons for which we know how they are connected is that we can have clear expectations about what we should see in optical imaging recordings in the context of the baseline settings (i.e. spontaneous activity in this case) of

the system. Naturally, this allows checking that the system level recordings (i.e. the simultaneous recording of neurons) are correct (i.e. there is no imaging or preparation induced artefact). Having an easy way to check the correctness of the optical recordings makes also easier to analyse any change in the joint activity of the recorded neurons due to changes in the recording conditions (e.g. effect of neuromodulators or sensory activity on neurons).

While the injection of individual neurons takes 20–30 min, the relative ease of maintaining the STG stable in the experimental setting allows in principle the filling of many neurons with dye. An alternative for the proposed method is to use micro-injection that may speed up the delivery of the dye into the neurons. We are also considering the use of other voltage-sensitive dyes that allow the dyeing of many neurons simultaneously by bathing the whole STG in dye solution (e.g. di-4-ANEPPS).

4.2. Understanding of emergent functionality of biological neural networks

The VSD imaging of STG neurons allows single-sweep recording of details of neural activities (e.g. IPSPs), reducing potential sources of computational errors and artefacts, and allowing the measurement of true details of neural interactions without filtering out of occasional outlier events, which otherwise may indicate significant events in the activity of the neuron and of the neural network (Figs. 5 and 6). Even more, it allows a single-event-based analysis, which contains more information than the average. Single action potential resolution has been achieved in a few systems, including the giant squid axon and the giant metacerebral neuron in helix (for summary see Baker et al., 2005). The spread of the action potentials within these large neurons was traced with photodiode arrays. Action potentials were recorded and elicited with microelectrodes, which also allowed the averaging of multiple trials to detect the action potentials. A successful demonstration of the detection of synaptic potentials with VSDs was given in a high-resolution study of the dendritic tuft of mitral cells in the olfactory bulb of the rat (Baker et al., 2005). Unlike single action potentials, EPSPs could only clearly be resolved when averaged. Individual action potentials could also be detected in cardiomyocytes (Bu et al., 2009; Warren et al., 2010), which are particularly suitable for these studies since they possess a rather slow time course.

In cell culture, it is rather easy to demonstrate the detection of action potentials and EPSPs. For example HEK293 cell culture is used as a test bed for new VSDs. Bradley et al. (2009) used the common tracer dye DiO (Cohen et al., 1974; Honig and Hume, 1986) as a fluorescent donor with dipicrylamine during laser spot illumination and were able to detect single PSPs through averaging. While this method is potentially very fast, it also disturbs the electrical properties of the cells by increasing the cell capacitance. Kuhn et al. (2004) used the VSD ANNINE-6 in HEK293 cells and showed that it possesses more than three times the signal-to-noise ratio of ANEP dyes. Yet, in *in vivo* recordings of the mouse barrel cortex only about a 1% change could be detected (Kuhn et al., 2008). FRET (Förster/fluorescence resonance energy transfer) dyes were also successfully used in HEK cells (Maher et al., 2007) and in pancreatic islets (Kuznetsov et al., 2005). While new microscope techniques are also promising (for example second harmonic generation microscopy; Dombeck et al., 2004; Nuriya et al., 2006) they have mostly been used for demonstration purposes. Functional studies involving the activities of individual neurons, in contrast, are rare. In an elegant study by Cacciatore et al. (1999) identified individual neurons involved in the initiation of swimming in leech were identified using FRET dyes and averaging over many trials. Yet, as is the case for the *aplysia* abdominal ganglion, in which up to 1000 individual cells can be imaged (Baker et al., 2005), the under-

lying circuitry is unknown, which makes a functional interpretation of the obtained results very difficult.

One of the reasons why central pattern generators are studied is their reliable and repetitive activity, but also the universal applicability of the mechanisms that drive them (Nusbaum and Beenhakker, 2002; Yuste et al., 2005; Marder and Bucher, 2007; Stein, 2009). It is because of this why the cellular and synaptic properties of many of these model circuits are well-known. Yet, the electrophysiological methods used in these preparations are insufficient to fulfill all requirements of current investigations, given the complex morphology of neurons and the homeostatic changes these neurons undergo during long-term measurements (Bucher et al., 2005). CPGs thus present themselves as ideal candidates for using VSD imaging. We here present the first example of the optical measurement of two individual neurons that synaptically interact in a functional central pattern generating circuit (Figs. 5 and 6). Not only were we able to derive the period of the network activity from the optical signal, we could also detect the phase-relationship between the LP and PD neurons. While the PDs belong to the pace-maker kernel of the CPG, LP provides the only feedback synapse from the follower network and accordingly can play a major role in rhythm generation (Thirumalai et al., 2006). We show that not only individual action potentials can be detected in single sweeps, but also that single IPSPs from the LP to PD feedback synapse and from PY neurons to LP are visible (Figs. 5E and 6). Since in many cases of other optical recordings extensive averaging and data post-processing is required (e.g. Cacciatore et al., 1999; Zecevic et al., 1989) the avoidance of these in the case of crab STG VSD imaging is important for understanding the details of true network dynamics (i.e. not only in an average or mean field sense, but in its actual fine details). We used low light levels and thus avoided the negative effects of photo-damage – in contrast to the use of lasers or high intensity light required for absorption imaging is much more likely to cause photo-damage (Sacconi et al., 2006; Karu, 1999). In addition, we were able to trace action potentials in the primary neurite (Fig. 4), providing an initial framework for future studies to monitor inter-cell interactions on a subcellular level in a functional environment.

While molecular approaches have gained much attention in recent years (e.g. Dickinson et al., 2009; Ma et al., 2009), the long-term measurement of simultaneous multi-neuron activity has been disregarded. This is despite the fact that the STG is a model system for the actions of neuromodulators, which often have long-term effects on their target circuits, and that the STG has lately been used to study the motor pattern recovery after nerve injury (Zhang et al., 2009). Our work opens new avenues for STG research allowing simultaneous and long-term recording of many STG neurons (in principle of all) in fine details (i.e. much faster recording than in the case of calcium imaging) and without requiring averaging of data over many trials. Imaging also removes the worry of losing the recording or damaging the neurons, which is typical in case of (long-term) intracellular recordings. This could allow the detailed study of functional recovery processes in the STG in previously impossible detail (e.g. tracking the changes of individual neurons as they resume their activity after losing the modulatory input to the STG from higher ganglia).

The effects of neuromodulators are well known for individual STG neurons (Harris-Warrick et al., 1995; Marder and Hooper, 1985; Ayali and Harris-Warrick, 1998; Gruhn et al., 2005; Johnson et al., 2005), however, the effects of these modulators (e.g. dopamine, serotonin) on the whole ganglion are known in much less detail. In particular, there is much to learn about the details of action mechanisms of neuromodulators on the CPGs that switch the behaviour of these, or switch the participation of certain neurons in them, or promote the synchronization or desynchronization of rhythms produced by different CPGs (Harris-Warrick et al., 1992;

Marder and Bucher, 2007). The combination with VSD imaging offers the opportunity to unravel the mysteries of the details of neuromodulation in the STG, due to the possibility of simultaneous tracking of the activity of multiple neurons in fine detail.

Intracellular recordings in the STG typically measure the membrane potential in the soma and thus report a somewhat pruned picture of the activity. Many fine details of neural interactions that happen in the neuropile (e.g. Ayali et al., 1998) may not be represented at the level of the soma or in axonal recordings. To gain a better understanding synaptic interactions and dynamics it would be helpful to also record neural events that happen in the neuropile using high magnification and high spatial resolution VSD imaging of selected dye filled neurons.

Finally, molecular studies of the STG (e.g. Dickinson et al., 2009; Ma et al., 2009) have revealed many details of STG neurons and opened up new possibilities for investigation of how these neurons work. The use of VSD imaging in combination with methods of molecular biology (e.g. over-expression or knock-out of channels or receptor molecules in selected neurons) has the potential to discover the role of molecular details of neurons in the context of STG neural dynamics.

VSD imaging of the STG has the potential to improve fundamentally our understanding of how the roles and interactions of neurons get dynamically determined in the context of a neural network. Since the STG is a relatively small, but still complex in behavioural terms, and also well-known in terms of details and connections of individual neurons, it offers an excellent test bed to create well-designed experiments aimed to untangle details of neural interactions in the context of emergence of network functionality. Better understanding of the emergent dynamics of the STG can help to improve the understanding of CPGs in general, and especially the understanding of interactions of CPGs. How does a single joint rhythm emerge from the orchestration of multiple CPGs? How does a CPG re-organize and restart its activity after losing its higher regulatory input? These and similar questions are very important in many areas of neuroscience, for example in understanding of motor control in the spinal cord (Grillner, 2006; Hagglund et al., 2010), motor control break-down in Parkinson's disease (Hausdorff et al., 2003), and also of higher cognitive functions (Yuste et al., 2005). VSD imaging of the STG can provide unprecedented detail about how the STG CPG get organized, how individual neurons get involved, to what extent are these neurons unique or interchangeable, and how the network behaviour emerges from interactions between individual neurons.

Appendix A. Supplementary data

Supplementary data associated with this article can be found, in the online version, at doi:10.1016/j.jneumeth.2010.10.007.

References

- Ayali A, Harris-Warrick RM. Interaction of dopamine and cardiac sac modulatory inputs on the pyloric network in the lobster stomatogastric ganglion. *Brain Res* 1998;794:155–61.
- Ayali A, Johnson BR, Harris-Warrick RM. Dopamine modulates graded and spike-evoked synaptic inhibition independently at single synapses in pyloric network of lobster. *J Neurophysiol* 1998;79:2063–9.
- Baker BJ, Kosmidis EK, Vucinic D, Falk CX, Cohen LB, Djuricic M, et al. Imaging brain activity with voltage- and calcium-sensitive dyes. *Cell Mol Neurobiol* 2005;25:245–82.
- Bartos M, Nusbaum MP. Intercircuit control of motor pattern modulation by presynaptic inhibition. *J Neurosci* 1997;17:2247–56.
- Blitz DM, Nusbaum MP. Motor pattern selection via inhibition of parallel pathways. *J Neurosci* 1997;17:4965–75.
- Bradley J, Luo R, Otis TS, DiGregorio DA. Submillisecond optical reporting of membrane potential in situ using a neuronal tracer dye. *J Neurosci* 2009;29:9197–209.
- Briggman KL, Abarbanel HDI, Kristan WB. Optical imaging of neuronal populations during decision-making. *Science* 2005;307:896–901.
- Briggman KL, Kristan WB. Imaging dedicated and multifunctional neural circuits generating distinct behaviors. *J Neurosci* 2006;26:10925–33.
- Briggman KL, Kristan WB, Gonzalez JE, Klienfeld D, Tsien RY. Monitoring integrated activity of individual neurons using FRET-based voltage-sensitive dyes. In: Canepari M, Zecevic D, editors. *Membrane Potential Imaging in the Nervous System*. Springer; 2010.
- Bu G, Adams H, Berbari EJ, Rubart M. Uniform action potential repolarization within the sarcolemma of in situ ventricular cardiomyocytes. *Biophys J* 2009;96:2532–46.
- Bucher D, Prinz AA, Marder E. Animal-to-animal variability in motor pattern production in adults and during growth. *J Neurosci* 2005;25:1611–9.
- Cacciatore TW, Brodfuehrer PD, Gonzalez JE, Jiang T, Adams SR, Tsien RY, et al. Identification of neural circuits by imaging coherent electrical activity with FRET-based dyes. *Neuron* 1999;23:449–59.
- Cohen LB, Salzberg BM, Davila HV, Ross WN, Landowne D, Waggoner AS, et al. Changes in axon fluorescence during activity: molecular probes of membrane potential. *J Membr Biol* 1974;19:1–36.
- Coleman MJ, Nusbaum MP, Cournil I, Claiborne BJ. Distribution of modulatory inputs to the stomatogastric ganglion of the crab *Cancer borealis*. *J Comp Neurol* 1992;325:581–94.
- Dickinson PS, Stemmler EA, Barton EE, Cashman CR, Gardner NP, Rus S, et al. Molecular, mass spectral, and physiological analyses of orcoxinins and orcoxinin precursor-related peptides in the lobster *Homarus americanus* and the crayfish *Procambarus clarkia*. *Peptides* 2009;30:297–317.
- Dombeck DA, Blanchard-Desce M, Webb WW. Optical recording of action potentials with second-harmonic generation microscopy. *J Neurosci* 2004;24:999–1003.
- Dombeck DA, Khabbaz AN, Collman F, Adelman TL, Tank DW. Imaging large-scale neural activity with cellular resolution in awake, mobile mice. *Neuron* 2007;56:43–57.
- Frost WN, Wang J, Brandon CJ. A stereo-compound hybrid microscope for combined intracellular and optical recording of invertebrate neural network activity. *J Neurosci Methods* 2007;162:148–54.
- Goulding M. Circuits controlling vertebrate locomotion: moving in a new direction. *Nat Rev Neurosci* 2009;10:507–18.
- Graubard K, Ross WN. Regional distribution of calcium influx into bursting neurons detected with arsenazo III. *Proc Natl Acad Sci* 1985;82:5665–9.
- Greenberg DS, Houweling AR, Kerr JND. Population imaging of ongoing neuronal activity in the visual cortex of awake rats. *Nat Neurosci* 2008;11:749–51.
- Grillner S. Biological pattern generation: the cellular and computational logic of networks in motion. *Neuron* 2006;52:751–66.
- Grinvald A, ZSalzberg BM, Cohen LB. Simultaneous recording from several neurones in an invertebrate central nervous system. *Nature* 1977;268:140–2.
- Gruhn M, Guckenheimer J, Land B, Harris-Warrick RM. Dopamine modulation of two delayed rectifier potassium currents in a small neural network. *J Neurophysiol* 2005;94:2888–900.
- Gutierrez GJ, Grashow RG. *Cancer borealis* stomatogastric nervous system dissection. *J Vis Exp* 2009, <http://www.jove.com/index/details.stp?id=1207>, doi:10.3791/1207.
- Hagglund M, Borgius L, Dougherty KJ, Kiehn O. Activation of groups of excitatory neurons in the mammalian spinal cord or hindbrain evokes locomotion. *Nat Neurosci* 2010;13:246–52.
- Harris-Warrick RM, Marder E, Selverston AI, Moulins, M, editors. *Dynamic Biological Networks. The Stomatogastric Nervous System*. Cambridge, MA: MIT Press; 1992.
- Harris-Warrick RM, Coniglio LM, Barazangi N, Guckenheimer J, Gueron S. Dopamine modulation of transient potassium current evokes phase shifts in a central pattern generator network. *J Neurosci* 1995;15:342–58.
- Hausdorff JM, Balash Y, Giladi N. Time series analysis of leg movements during freezing of gait in Parkinson's disease: akinesia, rhyme or reason? *Physica A* 2003;321:565–70.
- Heinzel HG, Weimann JM, Marder E. The behavioral repertoire of the gastric mill in the crab *Cancer pagurus*: an in situ endoscopic and electrophysiological examination. *J Neurosci* 1993;13:1793–803.
- Holekamp TF, Turaga D, Holy TE. Fast three-dimensional fluorescence imaging of activity in neural populations by objective-coupled planar illumination microscopy. *Neuron* 2008;57:661–72.
- Honig MG, Hume RI. Fluorescent carbocyanine dyes allow living neurons of identified origin to be studied in long-term cultures. *J Cell Biol* 1986;103:171–87.
- Hooper SL, DiCaprio RA. Crustacean motor pattern generator networks. *Neurosignals* 2004;13:50–69.
- Johnson BR, Schneider LR, Nadim F, Harris-Warrick RM. Dopamine modulation of phasing of activity in a rhythmic motor network: contribution of synaptic and intrinsic modulatory actions. *J Neurophysiol* 2005;94:3101–3111.
- Karu T. Primary and secondary mechanisms of action of visible to near-IR radiation on cells. *J Photochem Photobiol B: Biol* 1999;49:1–7.
- Kerr JND, de Kock CPJ, Greenberg DS, Bruno RM, Sakmann B, Helmchen F. Spatial organization of neuronal population responses in layer 2/3 of rat barrel cortex. *J Neurosci* 2007;27:13316–28.
- Khorkova O, Golowasch J. Neuromodulators, not activity, control coordinated expression of ionic currents. *J Neurosci* 2007;27:8709–18.
- Kuhn B, Fromherz P, Denk W. High sensitivity of Stark-shift voltage-sensing dyes by one- or two-photon excitation near the red spectral edge. *Biophys J* 2004;87:631–9.

- Kuhn B, Denk W, Bruno RM. *In vivo* two-photon voltage-sensitive dye imaging reveals top-down control of cortical layers 1 and 2 during wakefulness. *Proc Natl Acad Sci* 2008;105:7588–93.
- Kuznetsov A, Bindokas VP, Marks JD, Philipson LH. FRET-based voltage probes for confocal imaging: membrane potential oscillations throughout pancreatic islets. *Am J Physiol Cell Physiol* 2005;289:C224–9.
- Loew L. Potentiometric dyes: imaging electrical activity of cell membranes. *Pure Appl Chem* 1996;68:1405–9.
- Ma M, Szabo TM, Jia C, Marder E, Li L. Mass spectrometric characterization and physiological actions of novel crustacean C-type allatostatins. *Peptides* 2009;30:1660–8.
- Maher MP, Wu NT, Ao H. pH-insensitive FRET voltage dyes. *J Biomol Screen* 2007;12:656–67.
- Marder E, Bucher D. Understanding circuit dynamics using the stomatogastric nervous system of lobsters and crabs. *Annu Rev Physiol* 2007;69:291–316.
- Marder E, Hooper SL. Neurotransmitter modulation of the stomatogastric ganglion of decapods crustaceans. In: Selverston AI, editor. *Model Neural Networks and Behaviour*. Plenum Publishing Corporation; 1985. pp. 319–337.
- Marder E, Thirumalai V. Cellular, synaptic and network effects of neuromodulation. *Neural Netw* 2002;15:479–93.
- Marder E, Weimann JM. Modulatory Control of Multiple Task Processing in the Stomatogastric Nervous System. New York: Pergamon Press; 1992.
- Miller JP. Pyloric mechanisms. In: Selverston AI, Moulins M, editors. *The Crustacean Stomatogastric System*. Heidelberg: Springer-Verlag; 1987. p. 109–46.
- Milojkovic BA, Zhou W-L, Antic SD. Voltage and calcium transients in basal dendrites of the rat prefrontal cortex. *J Physiol* 2007;585(2):447–68.
- Mukamel EA, Nimmerjahn A, Schnitzer MJ. Automated analysis of cellular signals from large-scale calcium imaging data. *Neuron* 2009;63:747–60.
- Nuriya M, Jiang J, Nemet B, Eisenthal KB, Yuste R. Imaging membrane potential in dendritic spines. *Proc Natl Acad Sci* 2006;103:786–90.
- Nusbaum MP, Beenhakker MP. A small-systems approach to motor pattern generation. *Nature* 2002;417:343–50.
- Obaid AL, Koyano T, Lindstrom J, Sakai T, Salzberg BM. Spatiotemporal patterns of activity in an intact mammalian network with single-cell resolution: optical studies of nicotinic activity in an enteric plexus. *J Neurosci* 1999;19:3073–93.
- Ohki K, Chung S, Ch'ng YH, Kara P, Reid RC. Functional imaging with cellular resolution reveals precise micro-architecture in visual cortex. *Nature* 2005;433:597–603.
- O'Malley DM, Kao Y-H, Fetcho JR. Imaging the functional organization of zebrafish hindbrain segments during escape behaviors. *Neuron* 1996;17:1145–55.
- Orger MB, Kampff AR, Severi KE, Bollmann JH, Engert F. Control of visually guided behavior by distinct populations of spinal projection neurons. *Nat Neurosci* 2008;11:327–33.
- Ramirez J-M, Richter DW. The neuronal mechanism of respiratory rhythm generation. *Curr Opin Neurobiol* 1996;6:817–25.
- Ross WN, Graubard K. Spatially and temporally resolved calcium concentration changes in oscillating neurons of crab stomatogastric ganglion. *Proc Natl Acad Sci* 1989;86:1679–83.
- Rotschild G, Nelken I, Mizrahi A. Functional organization and polulation dynamics in the mouse primary auditory cortex. *Nat Neurosci* 2010;13:353–60.
- Sacconi L, Dombeck DA, Webb WW. Overcoming photodamage in second-harmonic generation microscopy: real-time optical recording of neuronal action potentials. *Proc Natl Acad Sci* 2006;103:3124–9.
- Sjulson L, Miesenbock G. Rational optimization and imaging *in vivo* of a genetically encoded optical voltage reporter. *J Neurosci* 2008;28:5582–93.
- Stein W. Modulation of stomatogastric rhythms. *J Comp Physiol A: Neuroethol Sens Neural Behav Physiol* 2009;195:989–1009.
- Stein W, Andras P. Light-induced effects of a fluorescent voltage-sensitive dye on neuronal activity in the crab stomatogastric ganglion. *J Neurosci Methods* 2010;188:290–4.
- Stein W, Smarandache CR, Nickmann M, Hedrich UB. Functional consequences of activity-dependent synaptic enhancement at a crustacean neuromuscular junction. *J Exp Biol* 2006;209:1285–300.
- Stosiek C, Garaschuk O, Holthoff K, Konnerth A. *In vivo* two-photon calcium imaging of neuronal networks. *Proc Natl Acad Sci* 2003;100:7319–24.
- Thirumalai V, Prinz AA, Johnson CD, Marder E. Red pigment concentrating hormone strongly enhances the strength of the feedback to the pyloric rhythm oscillator but has little effect on pyloric rhythm period. *J Neurophysiol* 2006;95:1762–70.
- Warren M, Spitzer KW, Steadman BW, Rees TD, Venable PW, Taylor T, et al. High precision recording of the action potential in isolated cardiomyocytes using the near-infrared fluorescent dye di-4-ANBDQBS. *Am J Physiol Heart Circ Physiol* 2010. doi:10.1152/ajpheart.00248.2010.
- Wu J-Y, Cohen LB, Falk CX. Neuronal activity during different behaviors in aplysia: a distributed organization? *Science* 1994;263:820–3.
- Yaksi E, von Saint Paul F, Niessing J, Bundschuh ST, Friedrich RW. Transformation of odor representations in target areas of the olfactory bulb. *Nat Neurosci* 2008;12:474–82.
- Yuste R, MacLean JN, Smith J, Lansner A. The cortex as a central pattern generator. *Nat Rev Neurosci* 2005;6:477–83.
- Zecevic D, Wu J-Y, Cohen LB, London JA, Höppf H.P., Falk CX. Hundreds of neurons in the Aplysia abdominal ganglion are active during the gill-withdrawal reflex. *J Neurosci* 1989;9:3681–9.
- Zhang Y, Khorkova O, Rodriguez R, Golowasch J. Activity and neuromodulatory input contribute to the recovery of rhythmic output after decentralization in a central pattern generator. *J Neurophysiol* 2009;101:372–86.
- Zhao S, Golowasch J, Nadim F. Pacemaker neuron and network oscillations depend on a neuromodulator-regulated linear current. *Front Behav Neurosci* 2010;18(4):21.